The structure of linkers affects the DNA binding properties of tethered dinuclear ruthenium (II) metallo-intercalators

Hiwa K Saeed[a], Ibrahim Q Saeed[b], Niklaas J Buurma[b], and Jim A. Thomas*[a]

[a] Department of Chemistry University of Sheffield Sheffield S3 7HF, UK
[b] Physical Organic Chemistry Centre, School of Chemistry, Cardiff University, Main Building Park Place, Cardiff CF10 3AT, UK

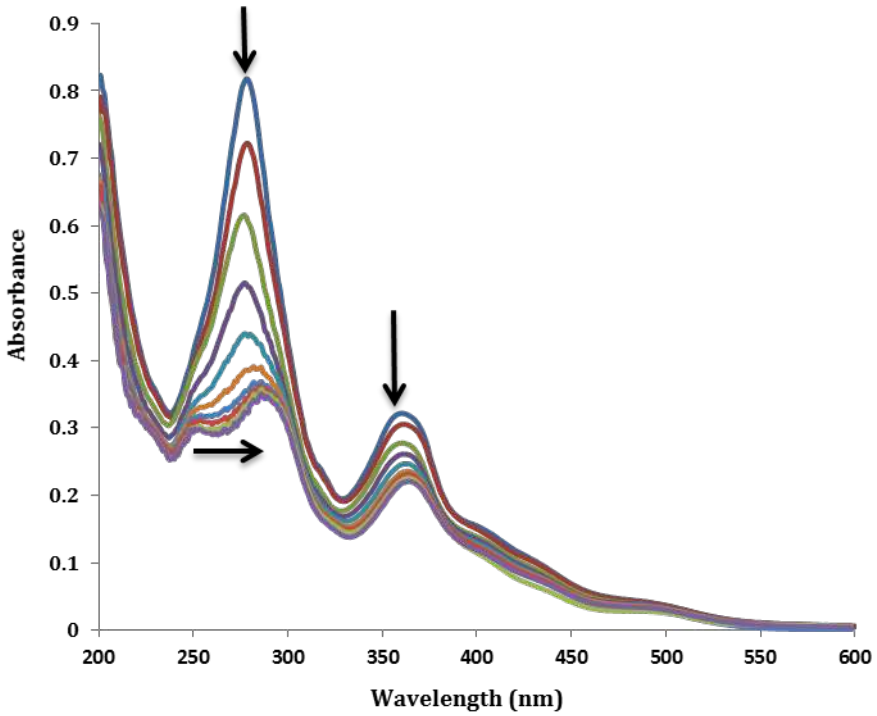

Fig S1. Corrected UV-visible spectra for 15 μM (initial concentration) solutions of chloride complex **8** on addition of CT-DNA in 5 mM tris buffer, 25 mM NaCl, pH 7.4 at 25 °C. For range of DNA concentrations, see Fig. 4 Top.

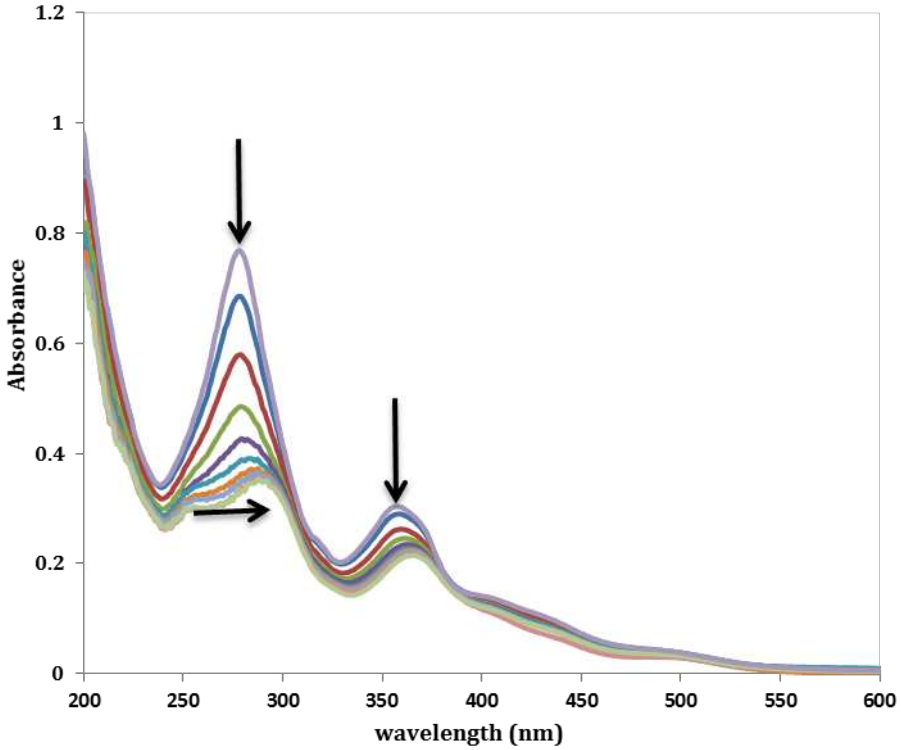

Fig S2. Corrected UV-visible spectra for 15 μM (initial concentration) solutions of chloride complex **10** on addition of CT-DNA in 5 mM tris buffer, 25 mM NaCl, pH 7.4 at 25 °C. For range of DNA concentrations, see Fig. S8.

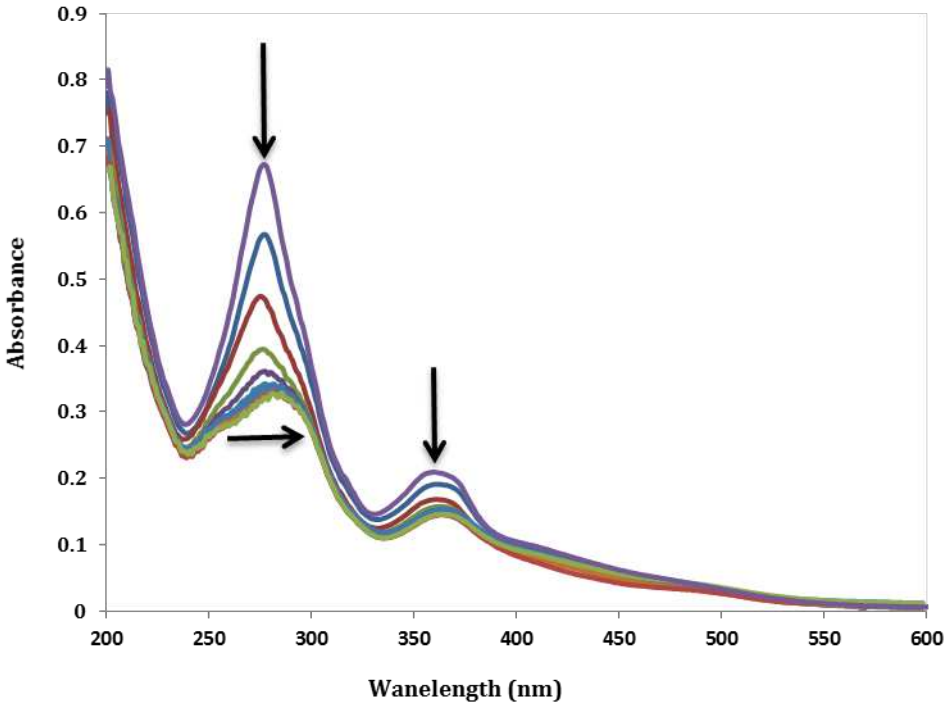

Fig S3. Corrected UV-visible spectra for 15 μM (initial concentration) solutions of chloride complex **11** on addition of CT-DNA in 5 mM tris buffer, 25 mM NaCl, pH 7.4 at 25 °C. For range of DNA concentrations, see Fig. S9.

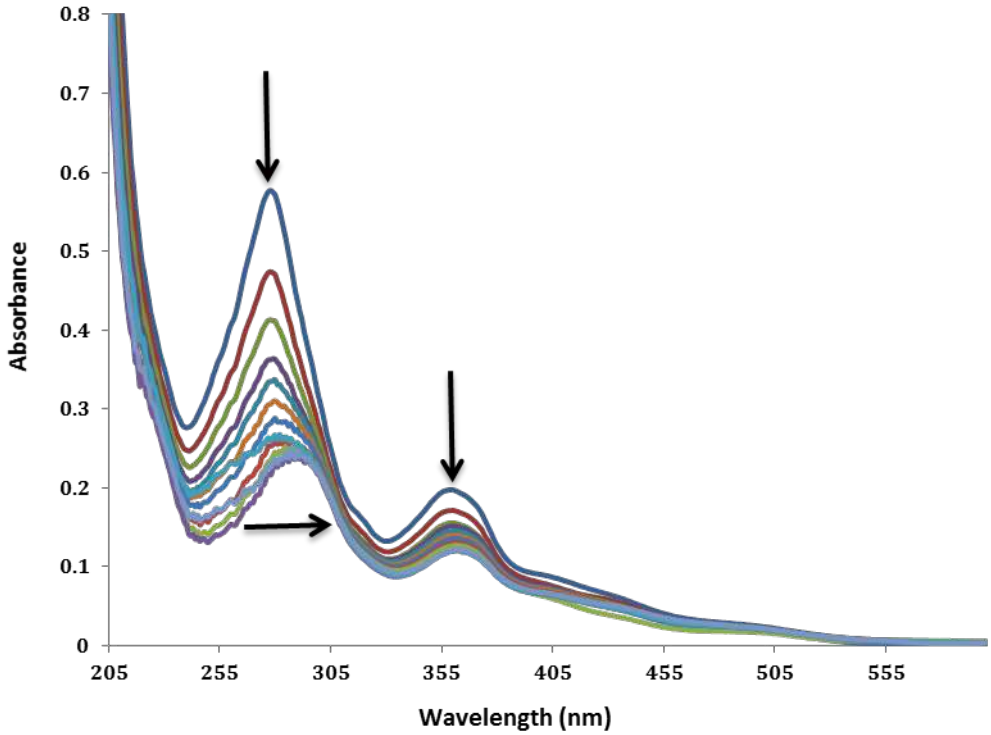

Fig S4. Corrected UV-visible spectra for 15 μM (initial concentration) solutions of chloride complex **12** on addition of CT-DNA in 5 mM tris buffer, 25 mM NaCl, pH 7.4 at 25 °C. For range of DNA concentrations, see Fig. 10.

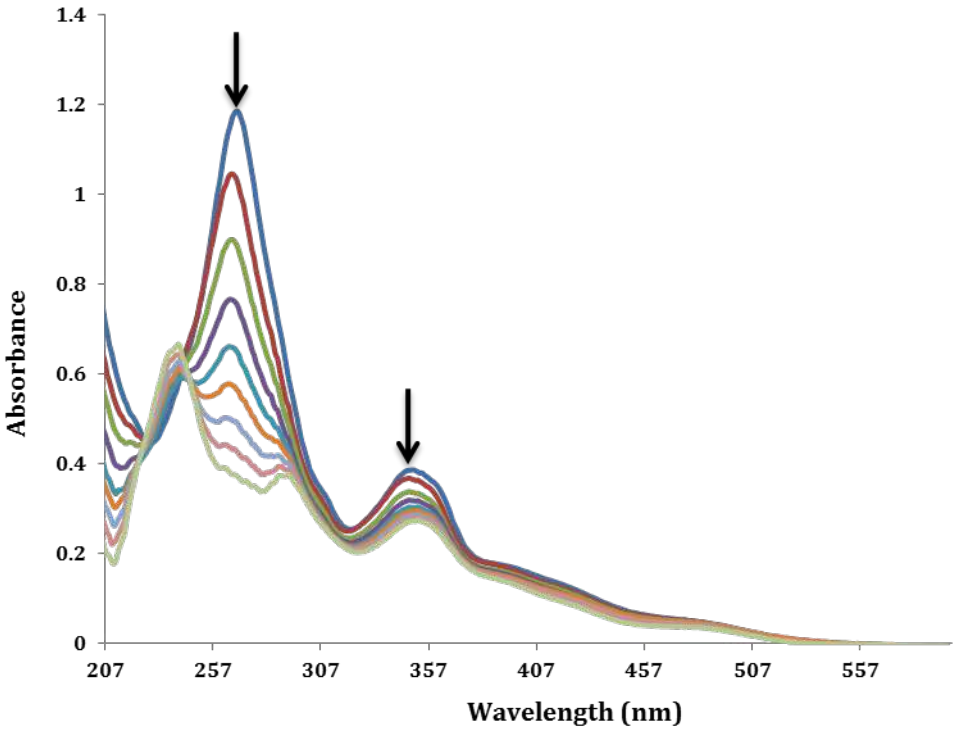

Fig S5. Corrected UV-visible spectra for 15 μM (initial concentration) solutions of chloride complex **13** on addition of CT-DNA in 5 mM tris buffer, 25 mM NaCl, pH 7.4 at 25 °C. For range of DNA concentrations, see Fig. S11.

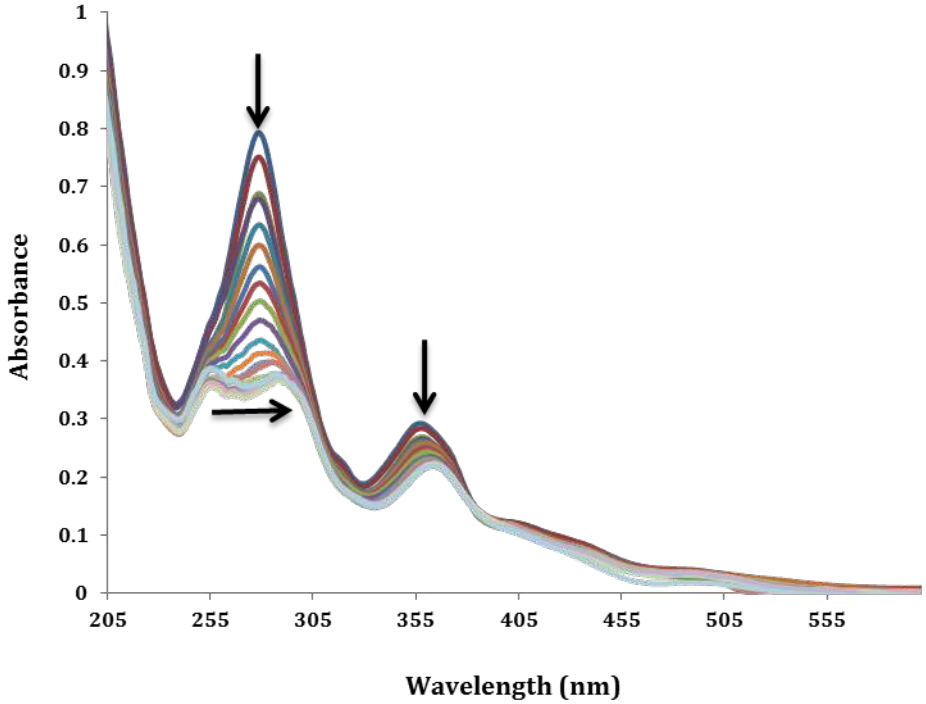

Fig S6. Corrected UV-visible spectra for 15 μM (initial concentration) solutions of chloride complex **14** on addition of CT-DNA in 5 mM tris buffer, 25 mM NaCl, pH 7.4 at 25 °C. For range of DNA concentrations, see Fig. S12.

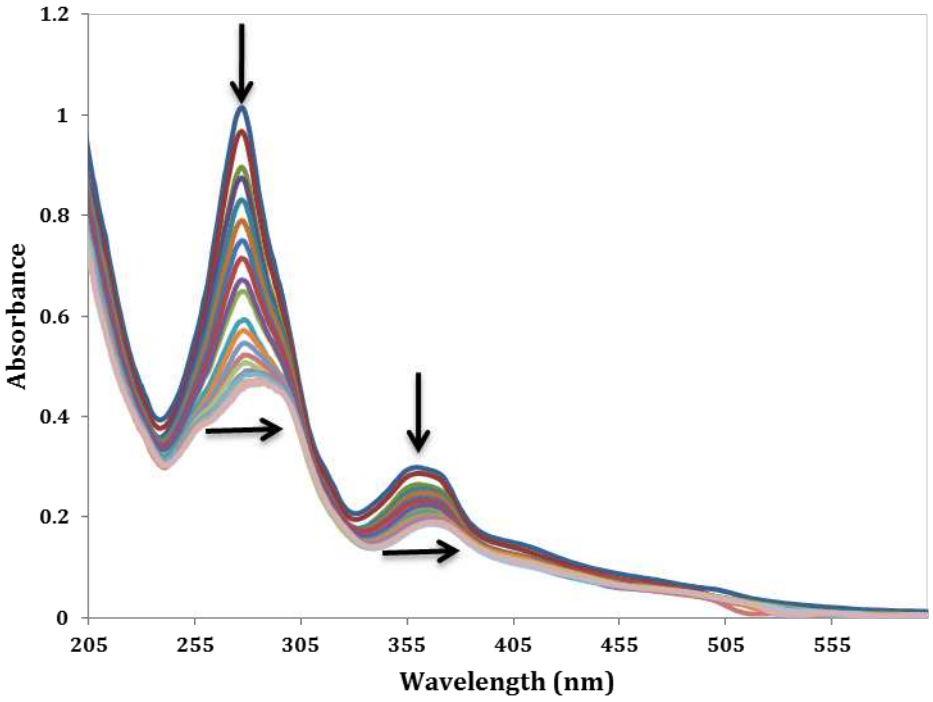

Fig S7. Corrected UV-visible spectra for 15 μM (initial concentration) solutions of chloride complex **15** on addition of CT-DNA in 5 mM tris buffer, 25 mM NaCl, pH 7.4 at 25 °C. For range of DNA concentrations, see Fig. S13.

Multiple independent binding sites (MIS) model

The multiple independent binding sites (MIS) model was used to analyse the spectroscopic data. In this model, the binding equilibrium is defined in terms of concentrations of binding sites. The concentration of binding sites is related to the concentration of basepairs via the binding site size of *n* basepairs as $[\text{binding sites}]_{tot} = [\text{DNA}]_{tot} / n$ and the binding equilibrium is defined as:

Where the concentration of the complex, [complex], is the concentration of bound ligand $[\text{L}]_{bound}$, which equals the concentration of occupied (bound) binding sites $[\text{binding sites}]_{bound}$. This gives the equilibrium constant as:

$$[\text{L}]_{bound} = K \cdot [\text{L}]_{free} \cdot [\text{binding sites}]_{free}$$

As shown elsewhere (Supporting Information for DOI: 10.1002/chem.201504934) the mass balance equation leads to a quadratic equation which is solved in the usual manner to give

$$[\text{L}]_{bound} = \left\{ \frac{1 + K \cdot \frac{[\text{DNA}]_{tot}}{n} + K \cdot [\text{L}]_{tot} - \sqrt{\left(1 + K \cdot \frac{[\text{DNA}]_{tot}}{n} + K \cdot [\text{L}]_{tot}\right)^2 - 4 \cdot K^2 \cdot \frac{[\text{DNA}]_{tot}}{n} \cdot [\text{L}]_{tot}}}{2 \cdot K} \right\}$$

as the only physically reasonable solution. This expression for $[\text{L}]_{bound}$, together with the Lambert-Beer law, gives the expression used for the analysis of the spectroscopic data:

$$signal_{obsd,i} = signal_{background} + signal_{free,m} \cdot [\text{L}]_{tot,i} + \Delta_{binding} signal_{m} \cdot \left\{ \frac{1 + K \cdot \frac{[\text{DNA}]_{tot,i}}{n} + K \cdot [\text{L}]_{tot,i} - \sqrt{\left(1 + K \cdot \frac{[\text{DNA}]_{tot,i}}{n} + K \cdot [\text{L}]_{tot,i}\right)^2 - 4 \cdot K^2 \cdot \frac{[\text{DNA}]_{tot,i}}{n} \cdot [\text{L}]_{tot,i}}}{2 \cdot K} \right\}$$

Here, $signal_{obsd}$ is the observed signal (absorption for UV/visible spectroscopy); $signal_{background}$ is the background signal (baseline UV/visible absorption of buffer and cuvette for UV/visible spectroscopy); $signal_{free,m}$ is the molar signal of the free ligand (extinction coefficient for UV/visible spectroscopy); $\Delta_{binding} signal_{m}$ is the change in the molar signal upon binding (change in the extinction coefficient for UV/visible spectroscopy); K is the equilibrium constant; $[\text{DNA}]_{tot,i}$ is the concentration of added DNA after injection i; N is the binding site size (defined as concentration of binding sites added = $[\text{DNA}]_{tot} / n$). Our equation further includes a term for the total concentration of the ligand after every injection i, $[\text{L}]_{tot,i}$, allowing analysis of data where the ligand concentration is not kept constant during the titration. This Equation is valid 1) for titrations carried out using spectroscopic detection methods (UV-visible, fluorescence and/or circular dichroism spectroscopy) at wavelengths where only the nucleic acid binder causes a signal and 2) for titration data which has been corrected for the increasing absorbance as a result of the added DNA.

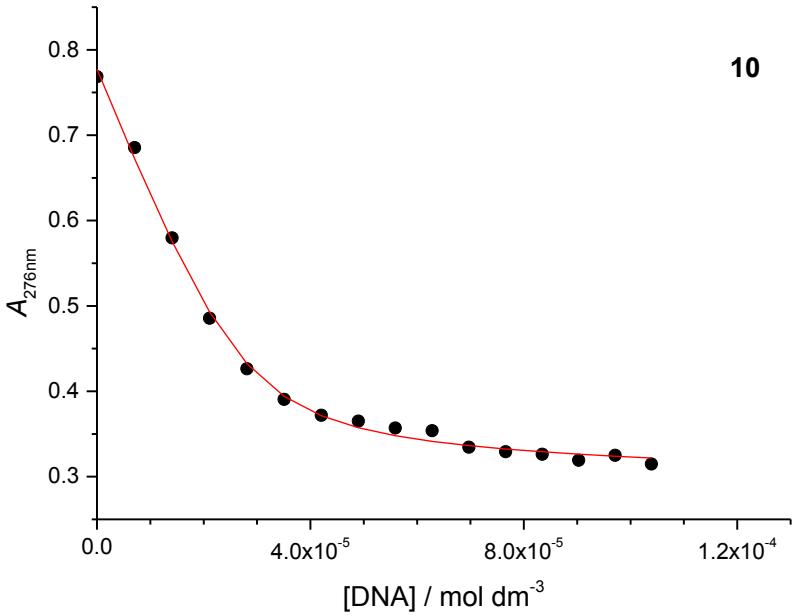

Fig S8. Fit of the MIS model to the UV-Visible spectroscopic titration data for complex **10**, • = data, — = fit.

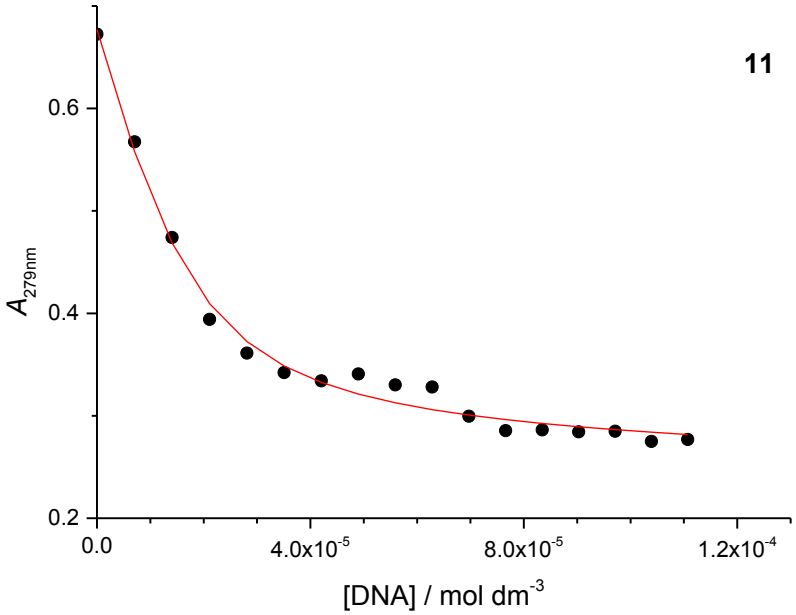

Fig S9. Fit of the MIS model to the UV-Visible spectroscopic titration data for complex **11**, • = data, — = fit.

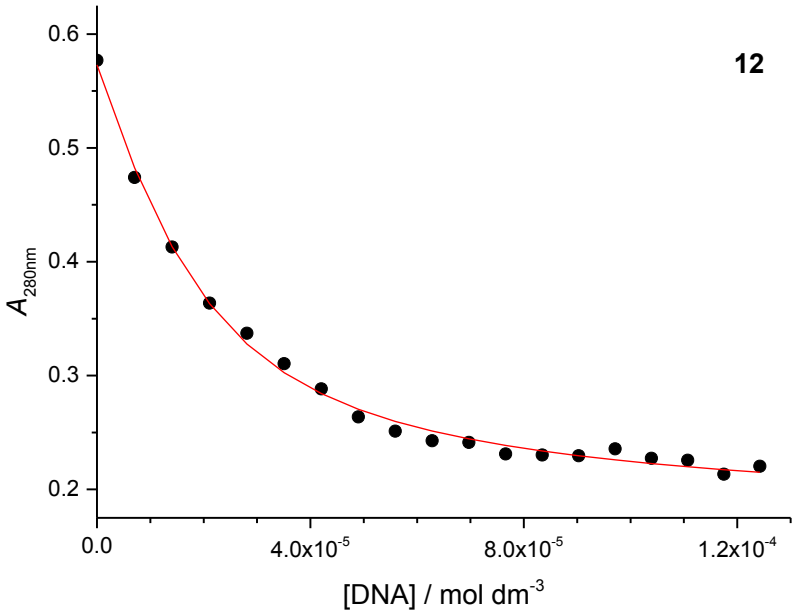

Fig S10. Fit of the MIS model to the UV-Visible spectroscopic titration data for complex **12**, • = data, — = fit.

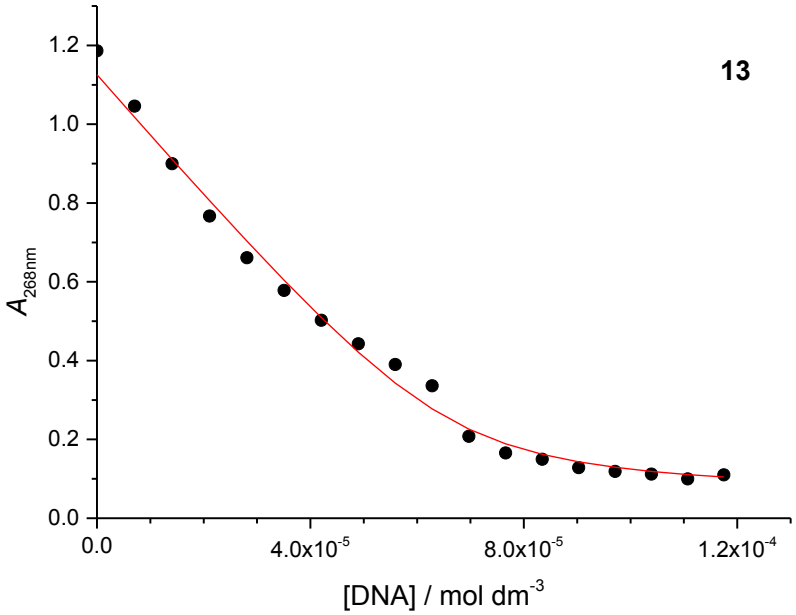

Fig S11. Fit of the MIS model to the UV-Visible spectroscopic titration data for complex **13**, • = data, — = fit.

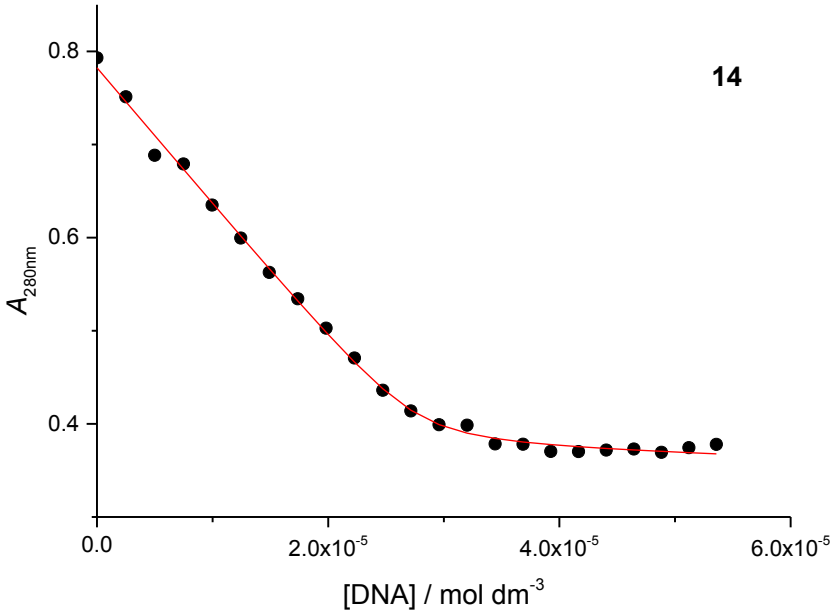

Fig S12. Fit of the MIS model to the UV-Visible spectroscopic titration data for complex **14**, • = data, — = fit.

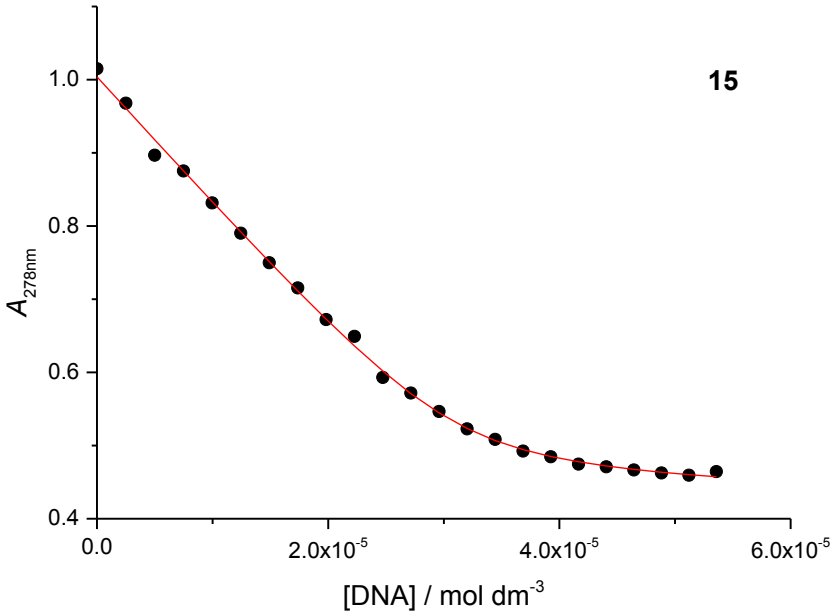

Fig S13. Fit of the MIS model to the UV-Visible spectroscopic titration data for complex **15**, • = data, — = fit.

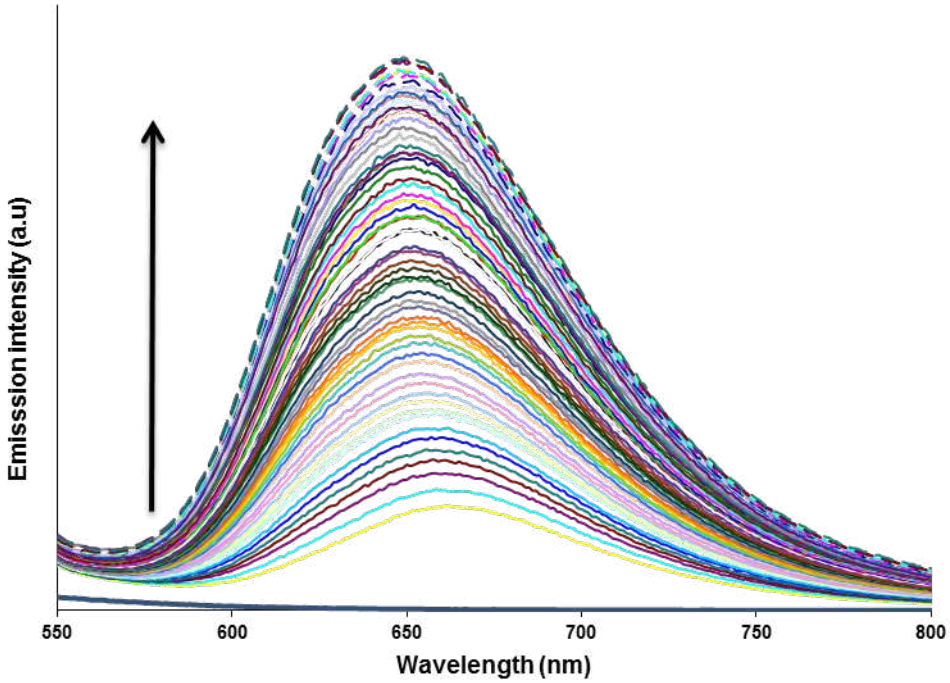

Fig S14. Luminescence spectra for titration of a 1.01 mM (in terms of basepairs) solution of CT-DNA into a solution of 15 μM [**8**]Cl_2 in 5 mM tris buffer, 25 mM NaCl, pH 7.4 at 25 °C.

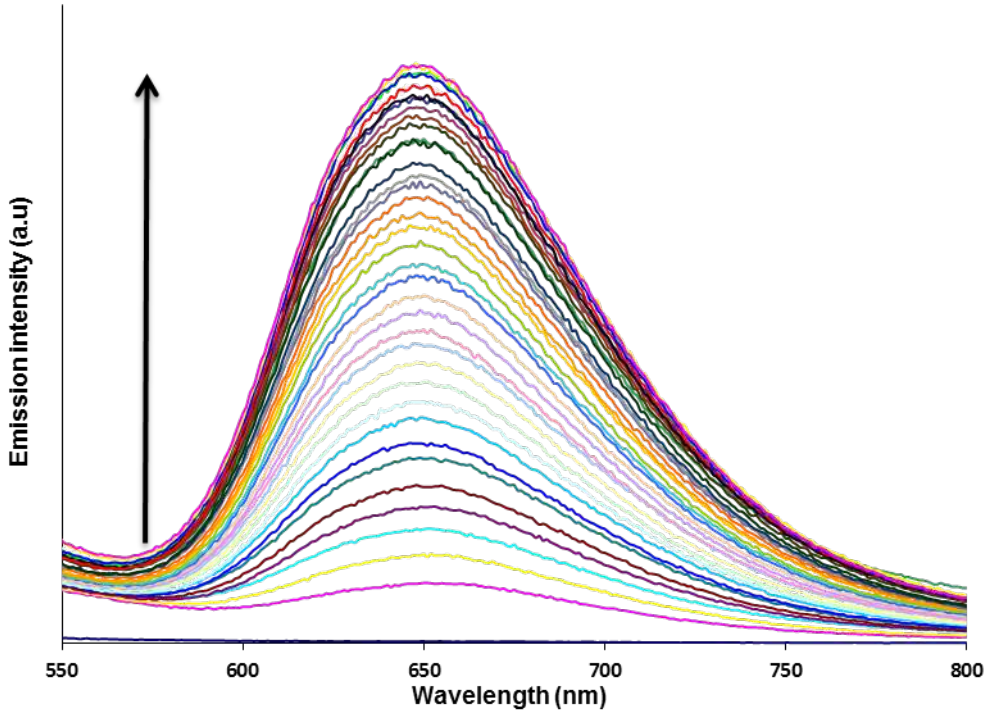

Fig S15. Luminescence spectra for titration of a 1.01 mM (in terms of basepairs) solution of CT-DNA into a solution of 15 μM [**10**]Cl_2 in 5 mM tris buffer, 25 mM NaCl, pH 7.4 at 25 °C.

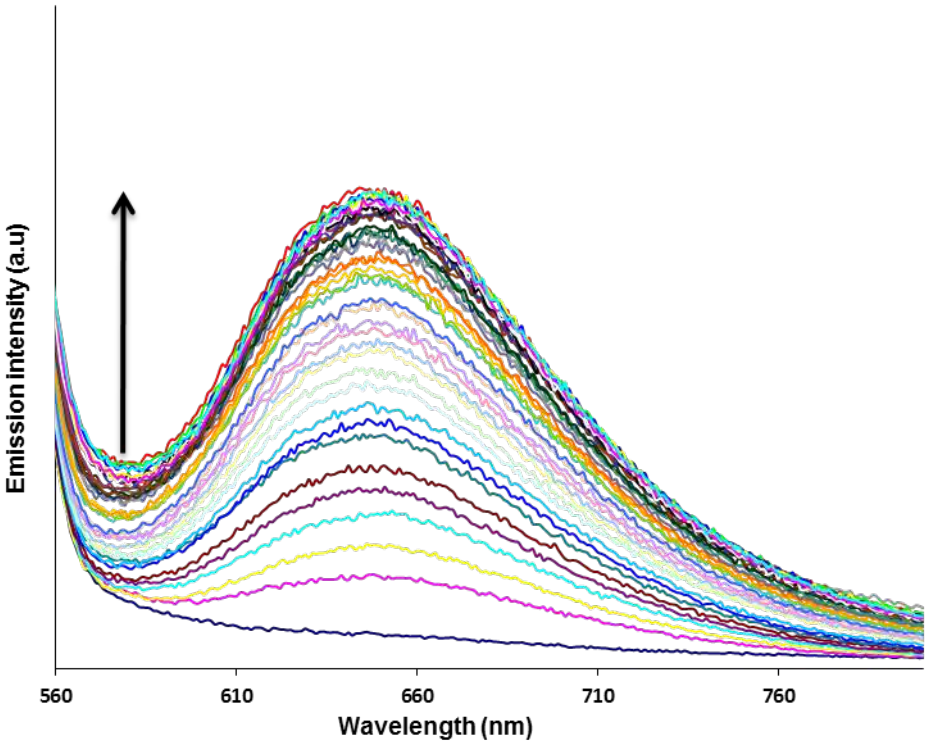

Fig S16. Luminescence spectra for titration of 1.01 mM (in terms of basepairs) solution of CT-DNA into a solution of 15 μM [**11**]Cl_4 in 5 mM tris buffer, 25 mM NaCl, pH 7.4 at 25 °C.

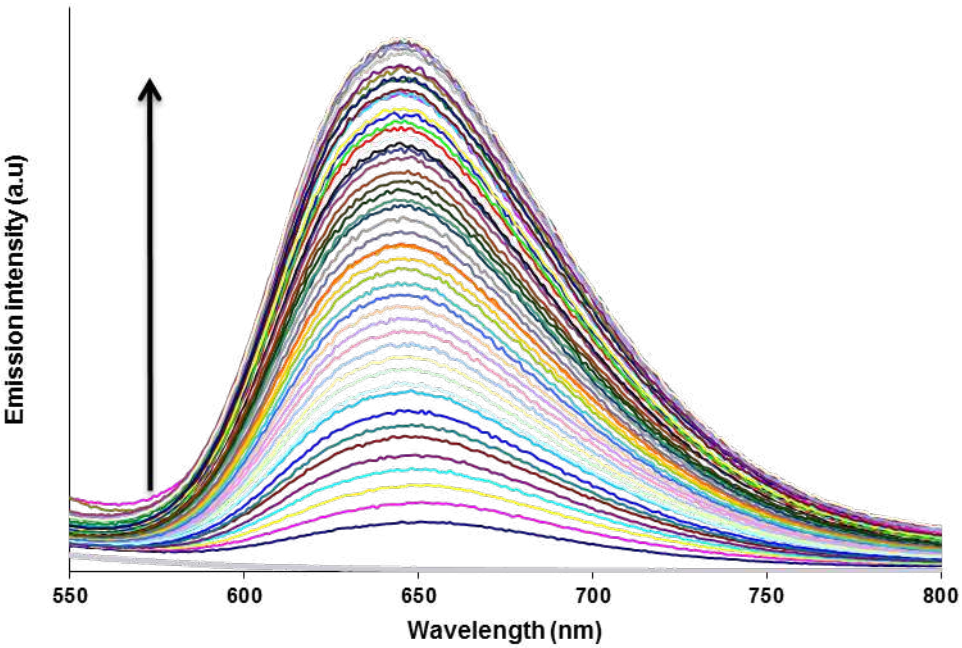

Fig S17. Luminescence spectra for titration of 1.01 mM (in terms of basepairs) solution of CT-DNA into a solution of 15 μM [**12**]Cl_2 in 5 mM tris buffer, 25 mM NaCl, pH 7.4 at 25 °C.

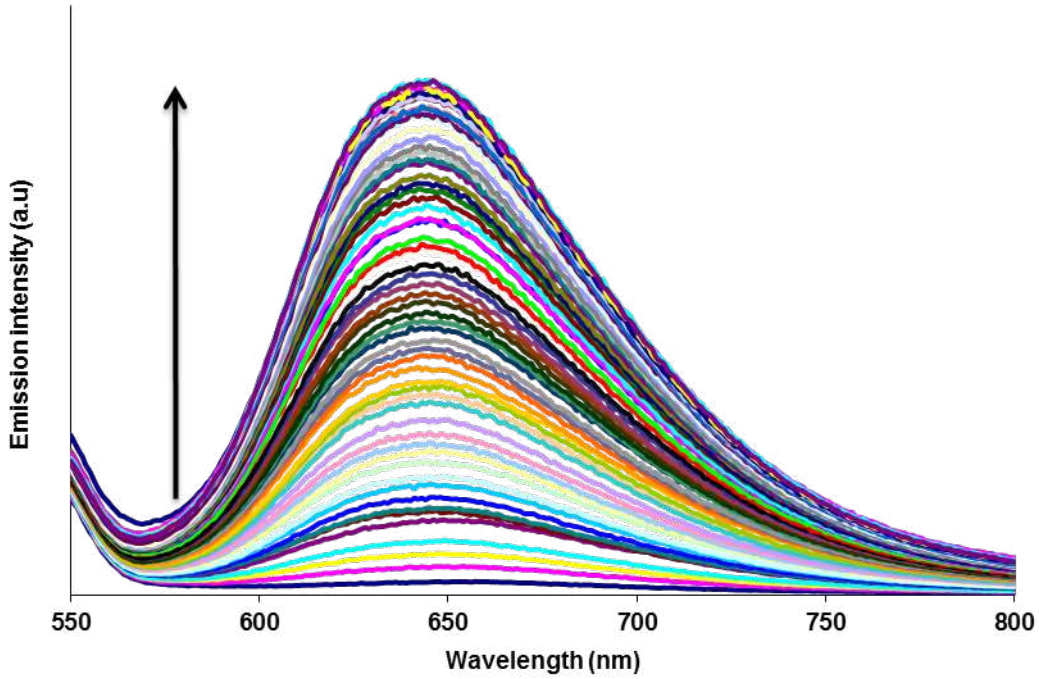

Fig S18. Luminescence spectra for titration of 1.01 mM (in terms of basepairs) solution of CT-DNA into a solution of 15 μM [**13**]Cl_4 in 5 mM tris buffer, 25 mM NaCl, pH 7.4 at 25 °C.

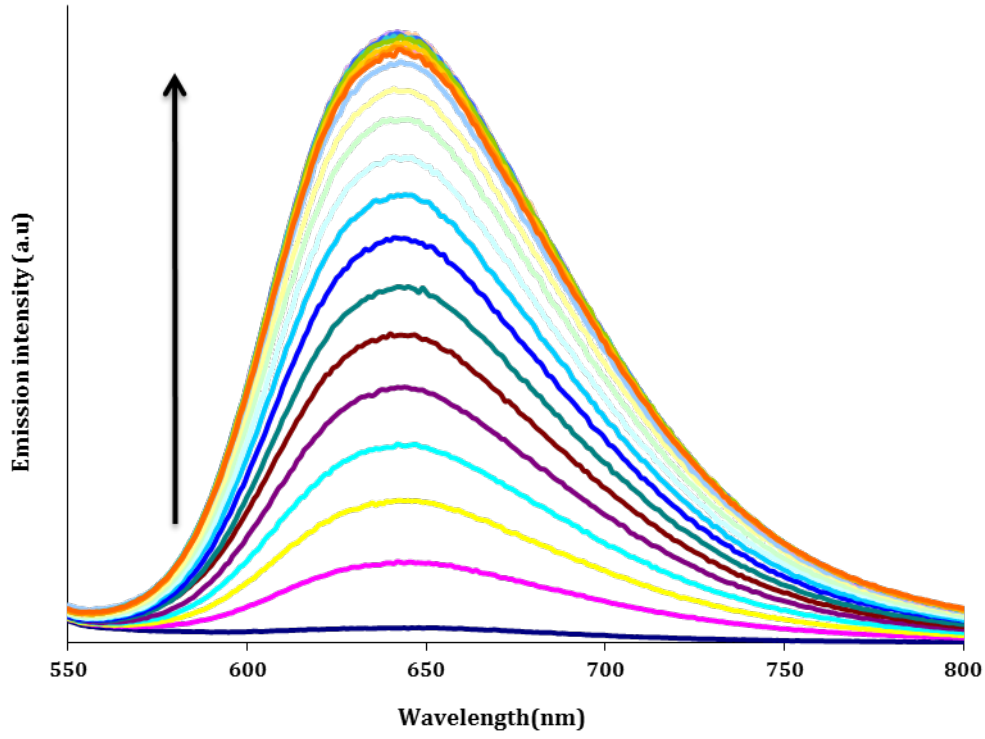

Fig S19. Luminescence spectra for titration of 1.01 mM (in terms of basepairs) solution of CT-DNA into a solution of 15 μM [**14**]Cl_2 in 5 mM tris buffer, 25 mM NaCl, pH 7.4 at 25 °C.

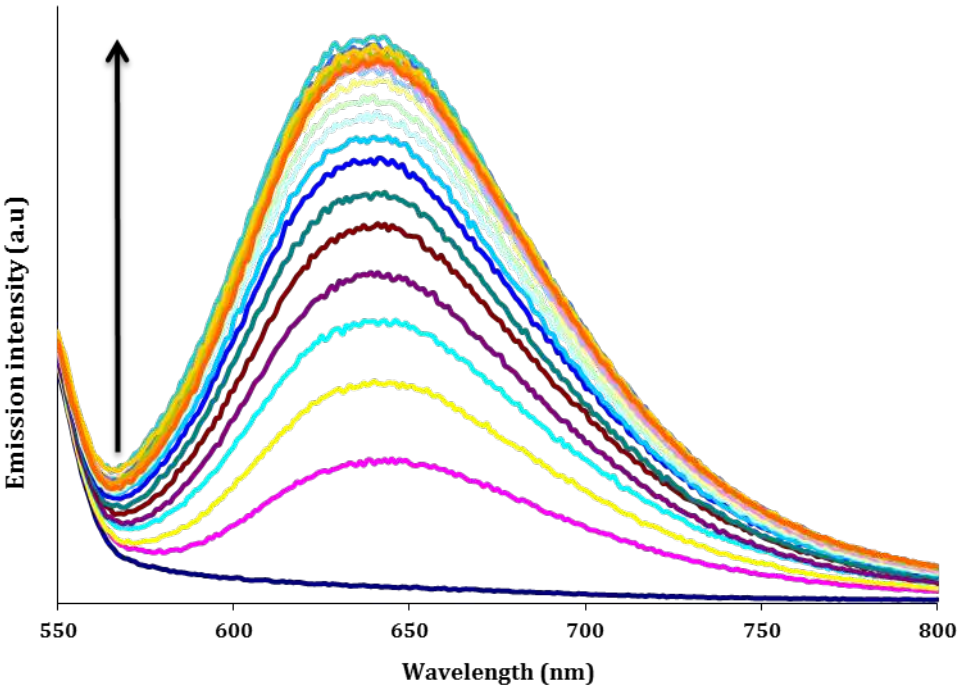

Fig S20. Luminescence spectra for titration of 1.01 mM (in terms of basepairs) solution of CT-DNA into a solution of 15 μM [**15**]Cl_4 in 5 mM tris buffer, 25 mM NaCl, pH 7.4 at 25 °C.

ITC data for complex 8

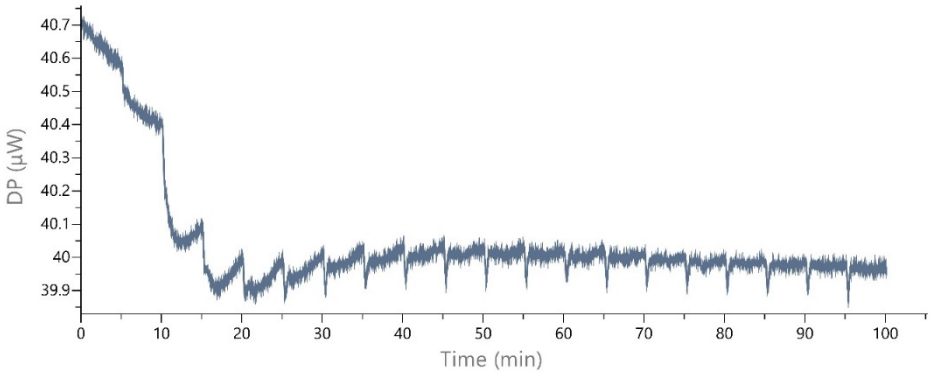

Fig S21A. Raw data for dilution of 1 mM **8**

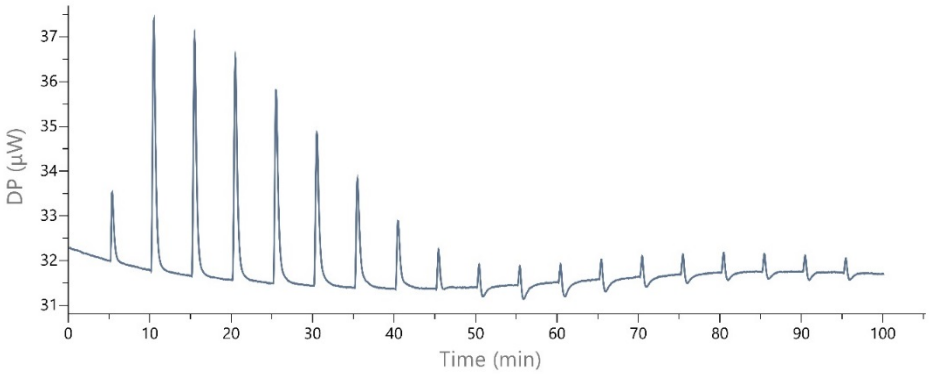

Fig S21B. Raw data for titration of 1 mM **8** into 250 µM CT-DNA

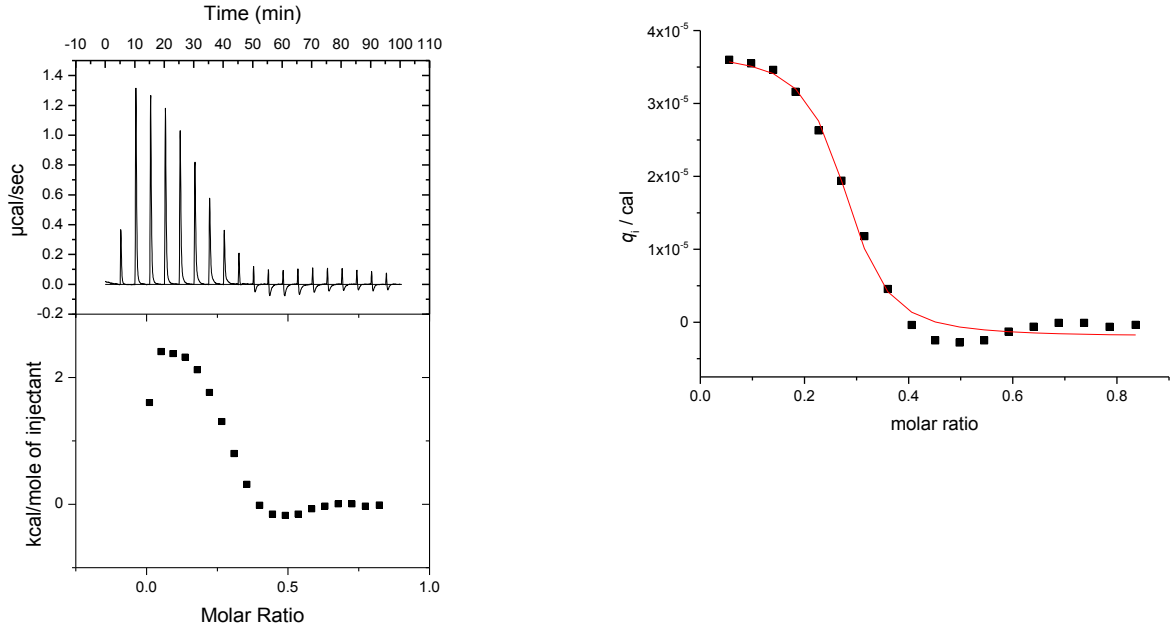

Fig S21C. Final figure and fitted heat effects for titration of 1 mM **8** into 250 µM CT-DNA

ITC data for complex 9

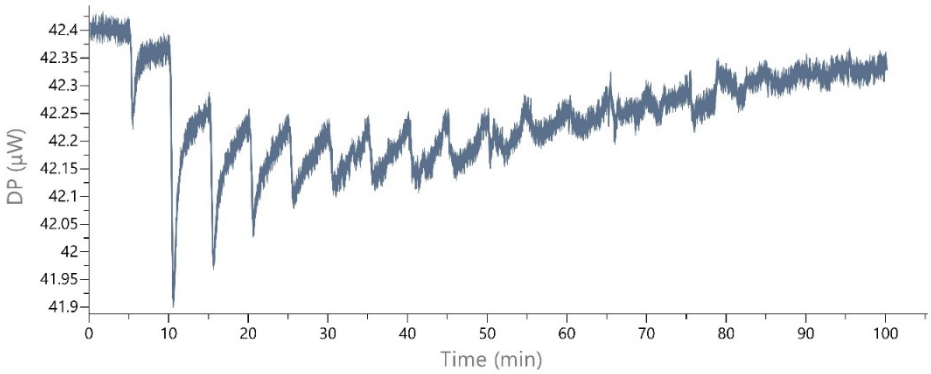

Fig S22A. Raw data for dilution of 1 mM **9**

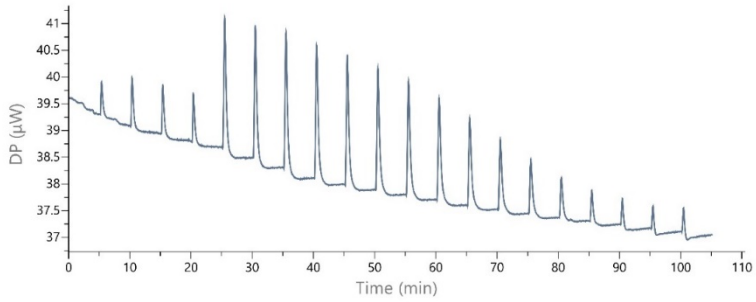

Fig S22B. Raw data for titration of 1 mM **9** into 250 µM CT-DNA

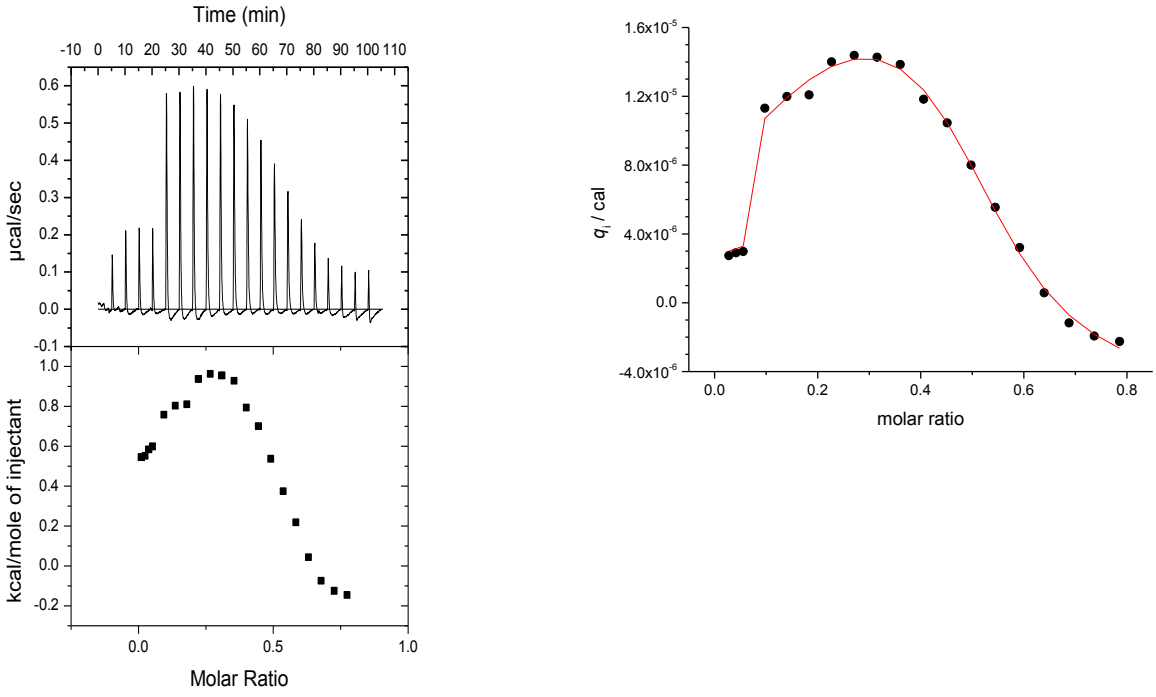

Fig S22C. Final figure and fitted heat effects for titration of 1 mM **9** into 250 µM CT-DNA

ITC data for complex 10

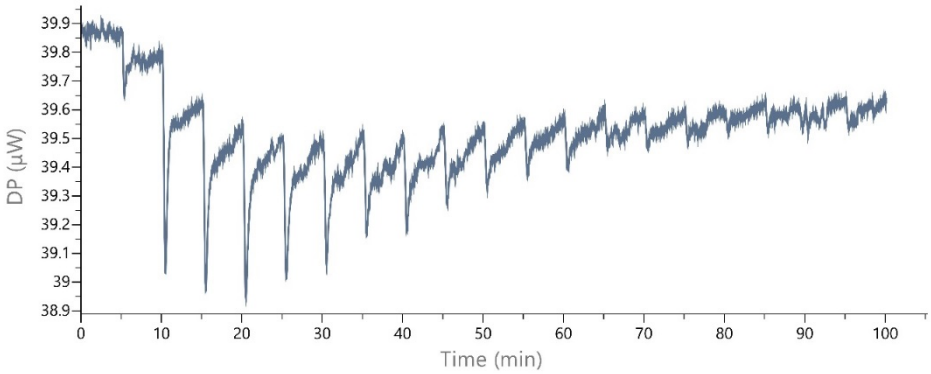

Fig S23A. Raw data for dilution of 1 mM **10**

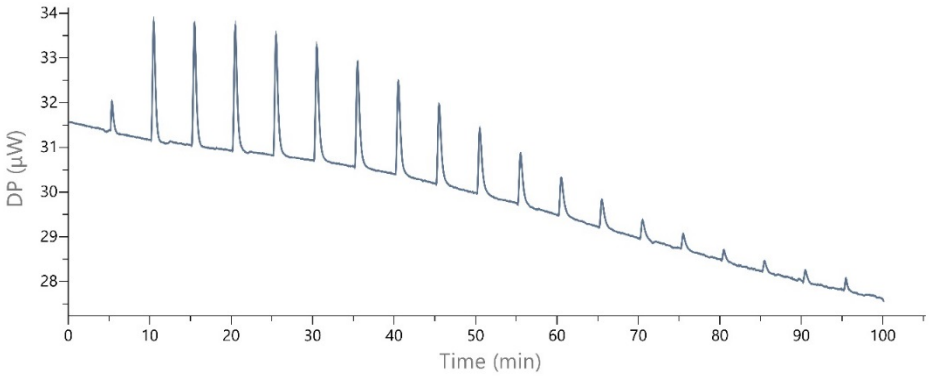

Fig S23B. Raw data for titration of 1 mM **10** into 250 µM CT-DNA

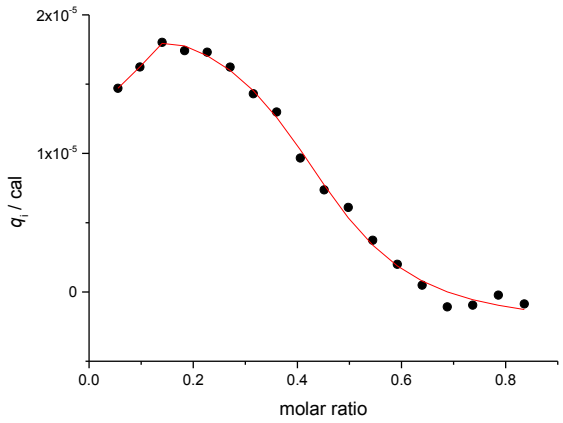

Fig S23C. Fitted heat effects for titration of 1 mM **10** into 250 µM CT-DNA

ITC data for complex 11

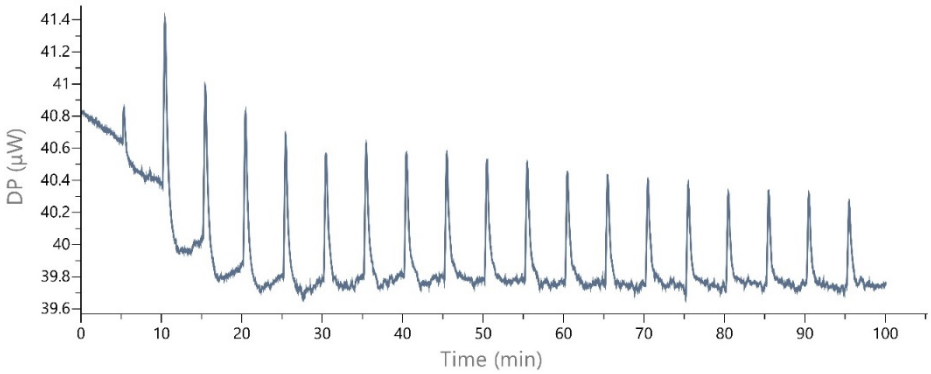

Fig S24A. Raw data for dilution of 1 mM **11**

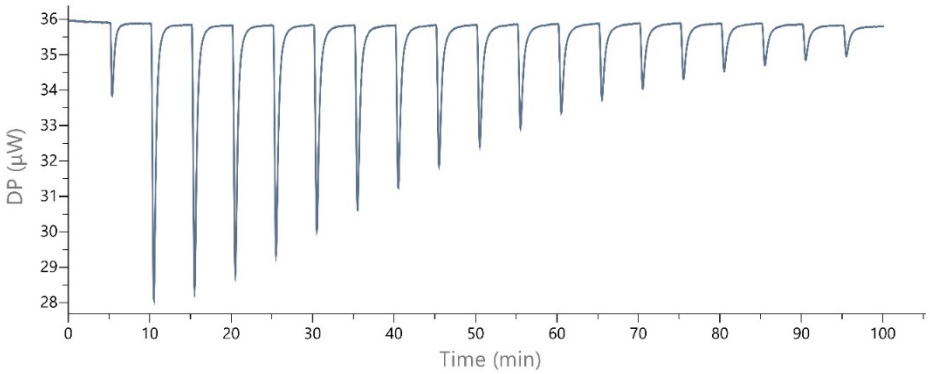

Fig S24B. Raw data for titration of 0.5 mM **11** into 125 µM CT-DNA

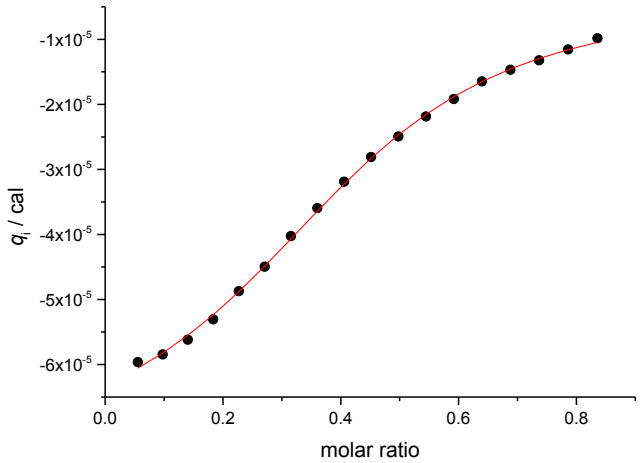

Fig S24C. Fitted heat effects for titration of 0.5 mM **11** into 125 µM CT-DNA

ITC data for complex 12

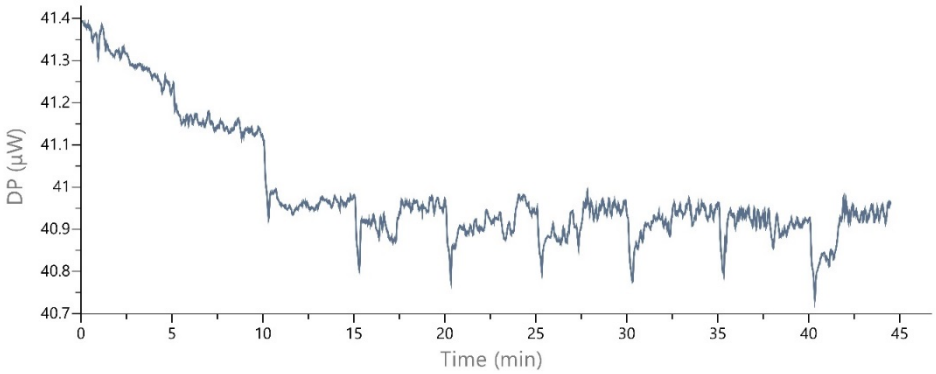

Fig S25A. Raw data for dilution of 1 mM **12**

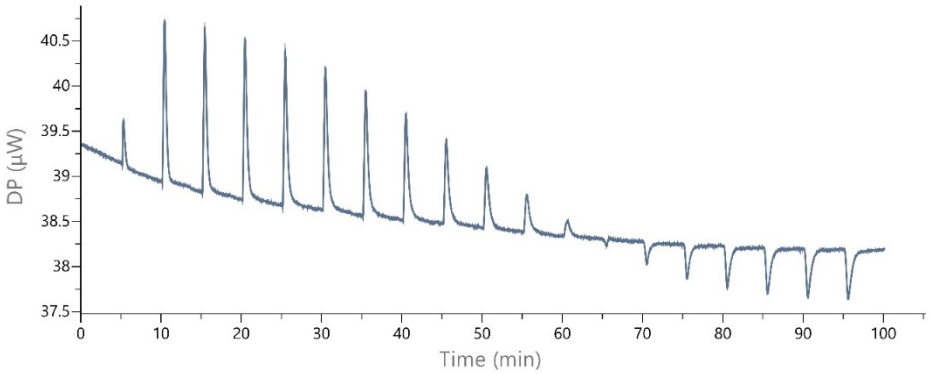

Fig S25B. Raw data for titration of 1 mM **12** into 250 µM CT-DNA

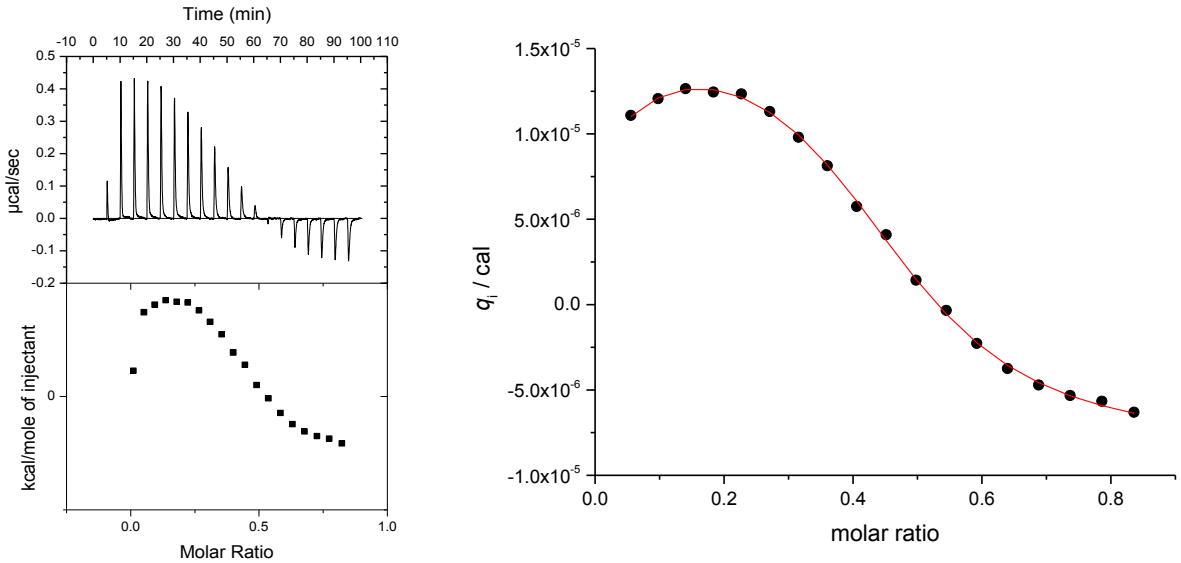

Fig S25C. Final figure and fitted heat effects for titration of 1 mM **12** into 250 µM CT-DNA

ITC data for complex 13

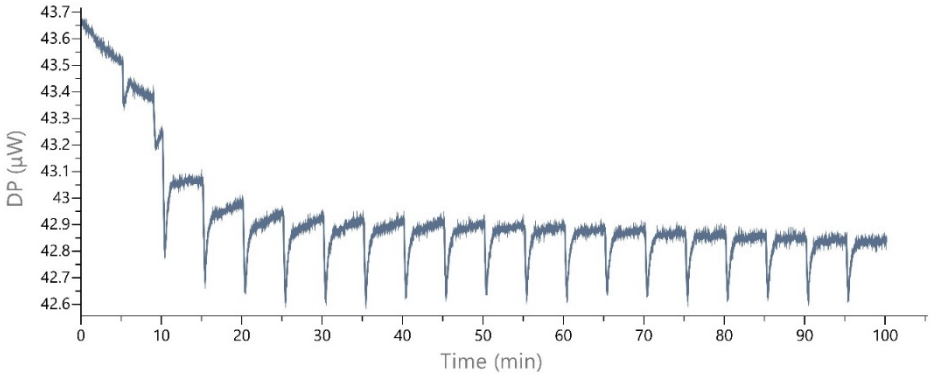

Fig S26A. Raw data for dilution of 1 mM **13**

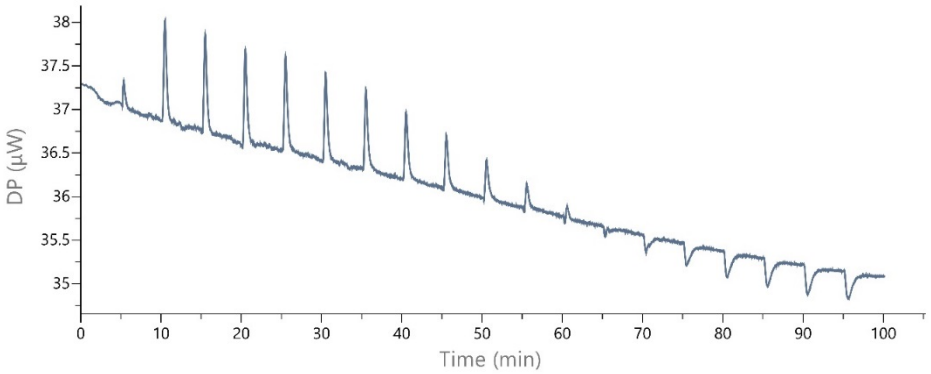

Fig S26B. Raw data for titration of 1 mM **13** into 250 µM CT-DNA

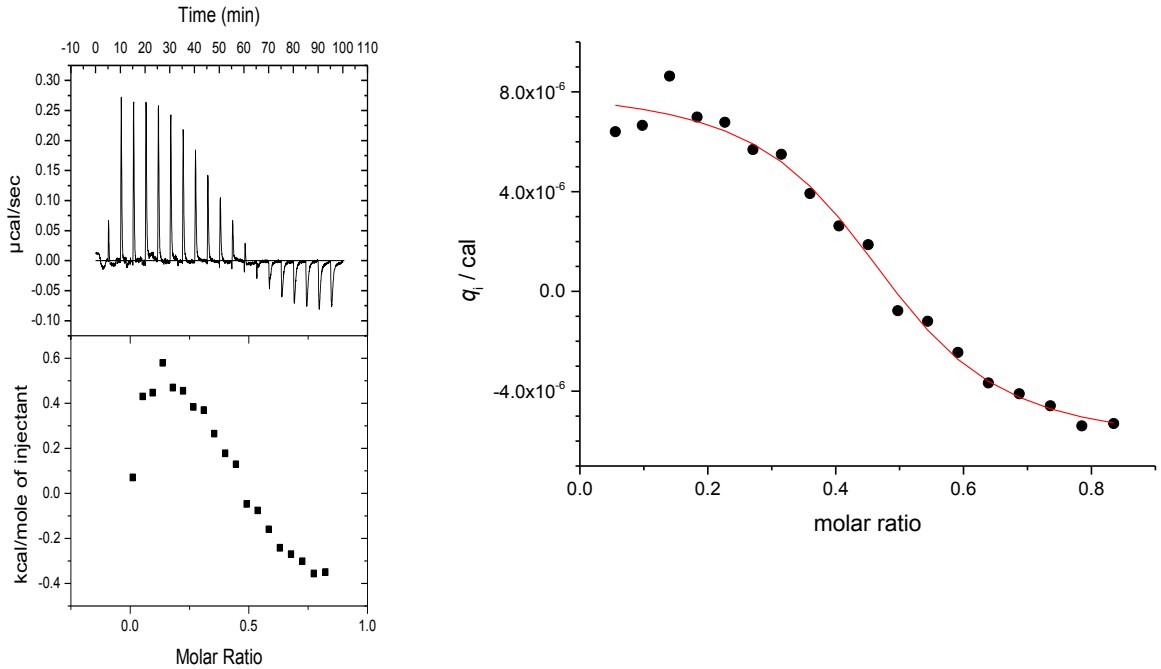

Fig S26C. Final figure and fitted heat effects for titration of 1 mM **13** into 250 µM CT-DNA

ITC data for complex 14

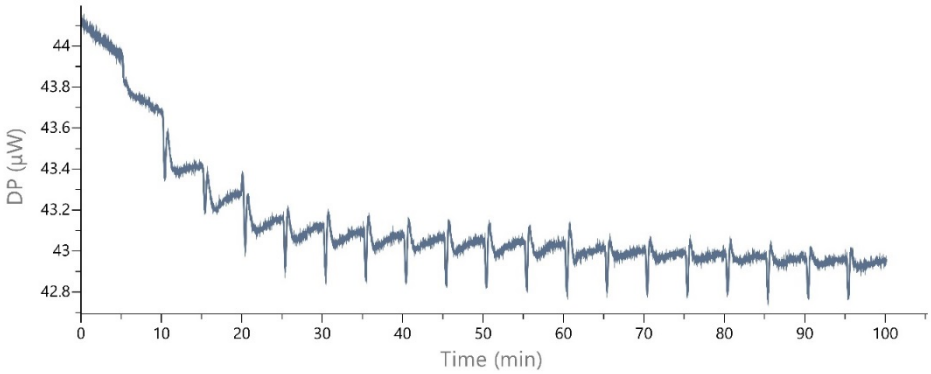

Fig S27A. Raw data for dilution of 1 mM **14**

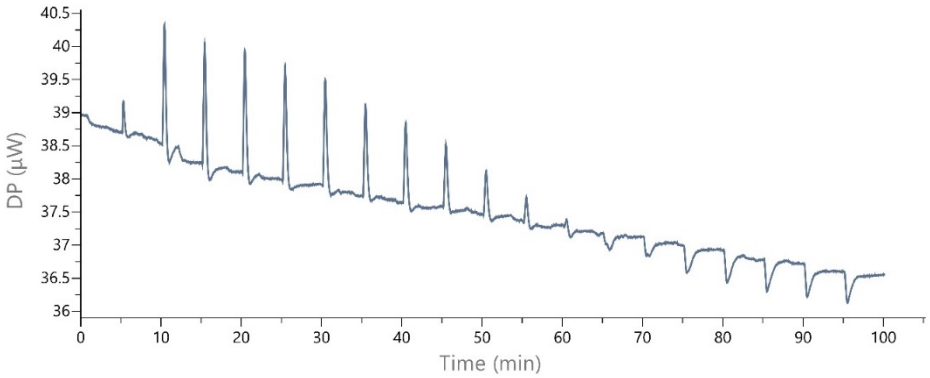

Fig S27B. Raw data for titration of 1 mM **14** into 250 µM CT-DNA

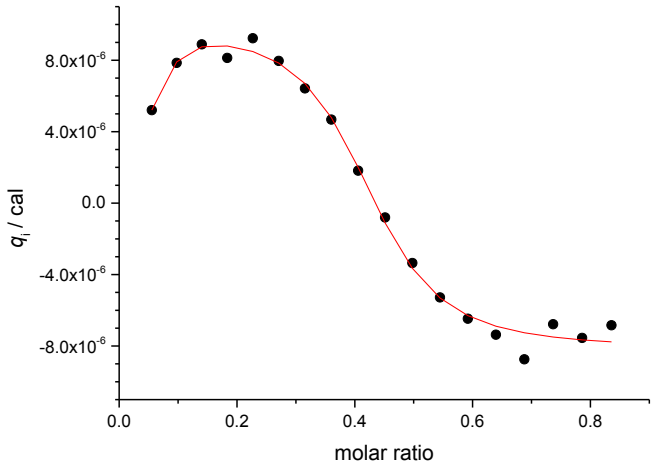

Fig S27C. Fitted heat effects for titration of 1 mM **14** into 250 µM CT-DNA

ITC data for complex 15

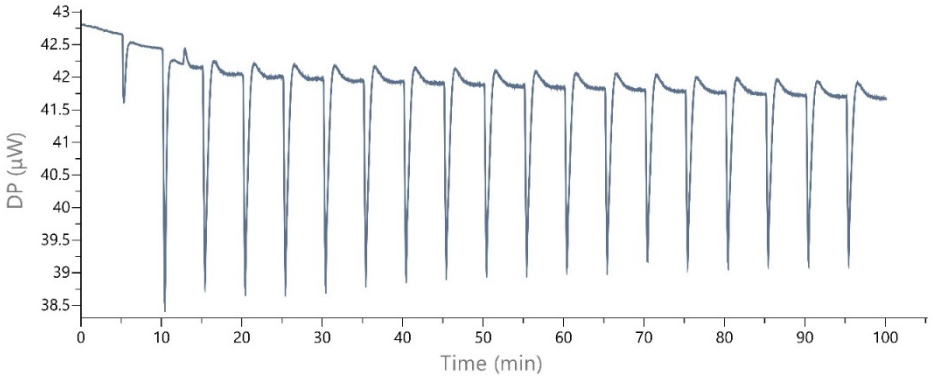

Fig S28A. Raw data for dilution of 1 mM **15**

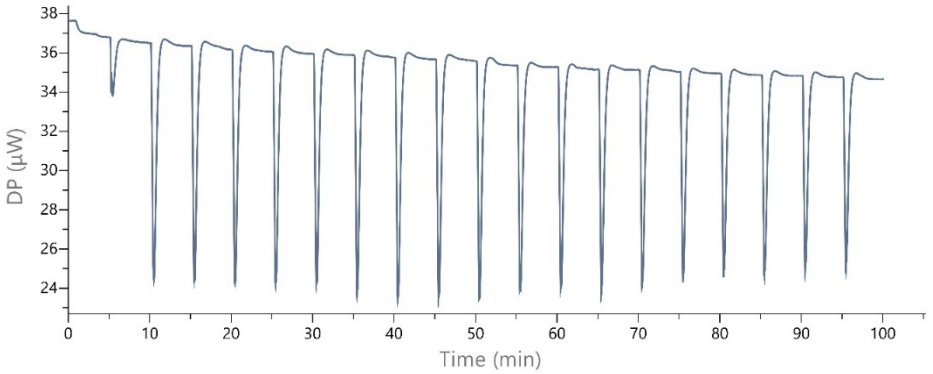

Fig S28B. Raw data for titration of 1 mM **15** into 250 µM CT-DNA

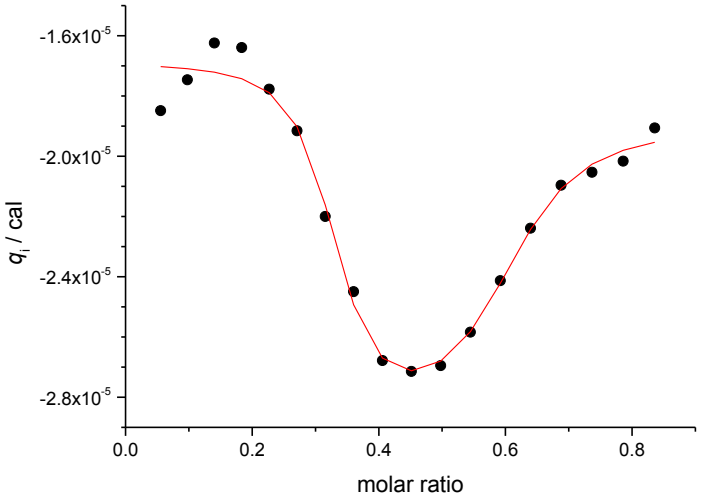

Fig S28C. Fitted heat effects for titration of 1 mM **15** into 250 µM CT-DNA